Research Square

Preprints are preliminary reports that have not undergone peer review.
They should not be considered conclusive, used to inform clinical practice,
or referenced by the media as validated information.

Clinical nodal findings and indocyanine green-guided sentinel node mapping in non-metastatic colon cancer: an exploratory prospective cohort stratified by postoperative mismatch-repair status

Teodor Staněk

teodor.stanek@mou.cz

Masaryk University

Zuzana Musilová

Masaryk University

Lukáš Fiala

Masaryk Memorial Cancer Institute

Svatava Janků

Masaryk Memorial Cancer Institute

Vuk Fait

Masaryk University

Research Article

Keywords: Colon cancer, Sentinel lymph node biopsy, Indocyanine green, Microsatellite instability, Mismatch repair, Neoplasm staging

Posted Date: August 26th, 2026

DOI: https://doi.org/10.21203/rs.3.rs-10568977/v1

License: This work is licensed under a Creative Commons Attribution 4.0 International License.
Read Full License

Additional Declarations: No competing interests reported.

Abstract

Background

Nodal enlargement can be difficult to interpret in mismatch-repair-deficient (dMMR) colon cancer, and indocyanine green-guided sentinel lymph node biopsy (ICG-SLNB) can miss nodal metastases. We described clinical nodal findings and ICG-SLNB results by postoperative mismatch-repair (MMR) status.

Methods

This exploratory, non-consecutive single-centre cohort included 40 patients undergoing elective colectomy for clinically non-metastatic colon cancer (May 2024 to March 2026). One radiologist retrospectively reread all CT scans, blinded to final pathological nodal status (pN) and MMR status. Against final composite pN we evaluated a binary ≥ 5-mm nodal-enlargement marker (CT-LAP), a study-defined size and morphology composite (CT-MTS), intraoperative lymphadenopathy and ICG-SLNB. MMR comparisons used exploratory Fisher exact tests. All diagnostic and MMR-stratified analyses were exploratory.

Results

MMR was available for 38 patients (14 dMMR; 24 mismatch-repair-proficient [pMMR]). CT-LAP was present in 14/14 dMMR and 7/24 pMMR tumours (difference + 70.8 percentage points, 95% CI 41.4 to 85.1; exploratory $p < 0.0001$), whereas pN-positive disease occurred in 7/14 and 6/24 (difference + 25.0 points, 95% CI − 5.6 to + 51.6; exploratory $p = 0.16$). Among pN-negative tumours, CT-LAP specificity was 0/7 in dMMR and 15/18 in pMMR (difference − 83.3 points, 95% CI − 94.2 to − 41.3). CT-MTS sensitivity was 46.2% (6/13) and specificity 92.0% (23/25). Sentinel-node detection succeeded in 38/40 patients (95.0%) and 36 invasive tumours were evaluable. Among 12 pN-positive patients with successful SLN detection, sensitivity was 50.0% (6/12, 95% CI 25.4 to 74.6) and negative predictive value 80.0% (24/30, 95% CI 62.7 to 90.5). One additional pN-positive dMMR patient had SLN non-detection. Ultrastaging found isolated tumour cells in six patients, but no micrometastasis and no pN-positive upstaging among 24 pN-negative patients with successful SLN detection (upper 95% limit 13.8%).

Conclusions

Every dMMR patient had at least one regional node ≥ 5 mm, but CT-LAP did not discriminate pN status within the dMMR stratum, and sensitivity after SLN detection was 50% under the study-specific ICG protocol. Selection, sparse strata and phenotype imbalances prevent attribution to MMR status or transfer of these estimates, and clinical benefit was not assessed. Validation in a consecutive, prespecified MMR-stratified cohort is required before these observations inform practice.

Trial registration:

Not registered.

Background

Final pathological nodal status (pN) is central to staging, prognosis and adjuvant treatment decisions in colon cancer, and adequate lymph-node retrieval is an established quality measure [1]. Nodal assessment nevertheless remains vulnerable to non-linear lymphatic spread and low-volume disease [2, 3]. Universal mismatch-repair (MMR) testing is now recommended in national colorectal cancer guidelines [4]. Testing of diagnostic biopsy specimens is feasible [5] and can inform Lynch syndrome assessment and surgical planning [6]. Preoperative MMR status has gained further relevance with the emergence of neoadjuvant immunotherapy for locally advanced dMMR colon cancer [7].

Preoperative CT has limited accuracy for nodal staging because size-based criteria can miss small metastases and can classify enlarged benign nodes as suspicious [8, 9]. Morphological features, including internal heterogeneity, can improve discrimination [10]. The size-based limitation is especially relevant in dMMR tumours, which are commonly right-sided and have an immune-rich microenvironment [11, 12]. dMMR tumours are also associated with higher lymph-node yields but, after stage adjustment, fewer nodal metastases than pMMR tumours [13, 14]. Published series report both overstaging and understaging by CT in dMMR colon cancer [8, 15]. These series did not, however, describe nodal enlargement and sentinel-node behaviour within the same MMR strata, so the interpretation of nodal enlargement in dMMR disease remains uncertain.

Sentinel lymph node biopsy (SLNB) has been evaluated as an adjunct to conventional pathological assessment after colectomy, including in prospective multicentre studies [16, 17]. It aims to select a limited number of nodes for intensive histopathological assessment and sensitive detection of low-volume disease [18–20]. Indocyanine green (ICG) enables real-time visualisation of lymphatic channels and candidate sentinel nodes [21, 22]. Detection rates are generally high, but variable sensitivity for nodal metastasis produces frequent false negatives [23–25]. A recent hypothesis-generating review responded to these limitations by calling for prospective sentinel-guided studies stratified by dMMR versus pMMR status [26].

Using a prospectively enrolled cohort, we addressed two linked exploratory questions. First, we used a blinded retrospective CT reread to record whether each patient had at least one regional node with a short-axis diameter ≥ 5 mm (CT-LAP). We then compared that finding across postoperative MMR strata. We separately described the patient-level classification of final pN by this deliberately sensitive enlargement marker, a study-defined CT-MTS composite and intraoperative lymphadenopathy. CT-LAP was not intended as a clinical metastatic threshold. Second, we estimated the ICG-SLNB detection rate and, among patients with a successfully detected sentinel node, the capture of pN-positive disease. We

also measured the yield of sentinel-node ultrastaging beyond routine pathology. All diagnostic-performance, subgroup and restriction analyses were exploratory.

Methods

Study design and setting

Reporting followed the Strengthening the Reporting of Observational Studies in Epidemiology (STROBE) statement, and the diagnostic component followed the Standards for Reporting of Diagnostic Accuracy Studies (STARD) 2015 statement [27, 28]. Completed checklists are provided as Additional files 2 and 3. This prospective observational cohort was conducted at the Department of Surgical Oncology, Masaryk Memorial Cancer Institute, Brno, Czech Republic, from May 2024 to March 2026. The ICG procedure and cohort data collection were prospective. The study CT interpretation was a retrospective blinded reread. Forty patients were analysed after two post-enrolment exclusions (Fig. 1).

The institutional Ethics Committee approved the protocol and final analysis (ref. 2024/1287/MOU, 7 May 2024), and all participants provided written informed consent. Enrolment was pragmatic, non-consecutive and dependent on the availability of the surgical team, and fluorescence system and on the operating theatre schedule. The study had no control arm, sample-size calculation, prespecified primary diagnostic estimand, clinical performance target, precision target or confirmatory hypothesis-testing framework. The available protocol was not publicly timestamped, so prespecification of the CT cut-offs, invasive-only diagnostic estimand and post-enrolment exclusions could not be independently verified.

Participants and MMR status

Eligible patients were adults undergoing elective oncological colectomy for biopsy-confirmed colonic adenocarcinoma, clinical stage cT1–cT4 and cM0. Eligibility was determined at enrolment. In one patient, a single hepatic metastasis identified at final pathology did not alter inclusion. Exclusion criteria were emergency surgery, neoadjuvant treatment, pregnancy or lactation, hypersensitivity to ICG or its formulation, and previous colonic resection within the same lymphatic basin.

An administrative theatre log identified 145 colonic resections coded as colon cancer (C18) during the study period, of which 42 underwent the ICG-SLNB protocol. Accordingly, 42/145 is not an enrolment fraction based on eligible patients, and the other 103 resections constitute a descriptive institutional surgical series rather than eligible non-enrolled controls.

Two protocol patients were excluded after final pathology. One had a neuroendocrine tumour discordant with the biopsy diagnosis. The available documentation did not distinguish biopsy sampling error from mixed histology. The other had dMMR colon cancer with an incidental complete pathological response (ypT0 ypN0) after immunotherapy for a synchronous non-colorectal malignancy. Both final diagnoses fell

outside the target population of untreated colonic adenocarcinoma. Both exclusions rested on target-population grounds and not on nodal status.

MMR status was determined by immunohistochemistry at final pathology and was therefore treated as a postoperative variable in every analysed case. A certified assay covering MLH1, PMS2, MSH2 and MSH6 was performed in a laboratory accredited to ISO 15189:2023. Tumours with MLH1 loss underwent MLH1 promoter methylation testing by bisulfite conversion followed by quantitative polymerase chain reaction (PCR). Testing was performed for every invasive carcinoma, so MMR status was unavailable only for the two pTis cases. The analysis extract retained the binary MMR classification but not individual protein-loss patterns or MLH1 methylation results. Therefore, sporadic and suspected hereditary dMMR could not be distinguished in this report. Stratified analyses were restricted to the 38 patients with known status. The preoperative dMMR result of the excluded immunotherapy-treated patient did not enter any analysis.

Sidedness was classified embryologically. Right-sided tumours extended from the caecum to the proximal two-thirds of the transverse colon, and left-sided tumours from the distal third of the transverse colon to the sigmoid colon.

Clinical nodal variables

A single radiologist retrospectively reread the preoperative imaging, blinded to final pN and MMR status, using size and morphology criteria informed by a colon cohort and a mixed colorectal cohort [10, 29]. Imaging comprised contrast-enhanced CT in 39 patients and positron emission tomography/computed tomography (PET/CT) in one patient. Only the CT component was evaluated. CT-LAP denoted the presence of at least one regional lymph node with a short-axis diameter ≥ 5 mm. It was a binary nodal-enlargement marker and did not measure node count, nodal stations, spatial distribution or total nodal volume. The study-defined CT-MTS composite denoted either a node > 10 mm or a 5–10 mm node judged qualitatively to be rounded and to show heterogeneous post-contrast enhancement.

The study record did not preserve the axis used for the > 10-mm arm, a numeric short-to-long-axis ratio for roundness or an attenuation threshold for heterogeneity. CT acquisition parameters, including contrast phase, slice thickness and reconstruction, were not abstracted into the analysis record. CT-to-resection intervals, repeat interval imaging, the timing of the reread relative to database review and the reader's access to the original clinical CT report were not retrievable from the study record.

The 5-mm threshold corresponds to the upper limit of normal short-axis diameter assigned by the Node Reporting and Data System (Node-RADS) to mesenteric-subregion nodes, for which enlargement without abnormal configuration carries only low suspicion [30]. In colon cancer, a 5-mm cut-off has shown 90% sensitivity for stage III disease at 31% specificity [10], so the present CT-LAP variable was used to describe enlargement rather than define metastatic disease. CT-MTS adopted a pragmatic size-and-morphology construction from the European Society of Gastrointestinal and Abdominal Radiology rectal

MRI consensus [31]. Morphology contributed only within the 5–10-mm window. Nodes > 10 mm were positive by size alone. The binary record did not retain morphology for every measurable node, and the images could not be rescored for size-independent internal heterogeneity without a new reread. As CT-MTS was nested within CT-LAP, all eight CT-MTS-positive cases were CT-LAP-positive. It is therefore a study-defined size-gated suspicion composite, not a validated colonic CT rule.

Intraoperative lymphadenopathy denoted one or more enlarged regional nodes or clustered nodal packets identified by consensus of the two operating surgeons. Open procedures allowed in vivo inspection and palpation, whereas robotic procedures allowed visual assessment only. Both approaches also included inspection and palpation of the resected specimen. The variable therefore combined operative and specimen-level information rather than representing a standardised, blinded intraoperative index test. No fixed threshold or independent adjudication was used, and the surgeons knew the preoperative CT findings. Specimen assessment could influence nodal retrieval, so the intraoperative lymphadenopathy variable was not independent of the subsequent pathological reference pathway.

ICG-guided SLNB and lymphatic mapping

Open or robot-assisted oncological colectomy was performed according to tumour location and institutional practice. After surgical access, Verdye ICG (Diagnostic Green GmbH, Aschheim-Dornach, Germany) was injected subserosally at 2.5 mg/mL in four peritumoural quadrants. The total volume was 2.5 mL, corresponding to 6.25 mg. Fluorescence was visualised with SPY-PHI (Stryker Corporation, Kalamazoo, MI, USA) in open procedures and da Vinci Firefly (Intuitive Surgical, Sunnyvale, CA, USA) in robotic procedures at 0, 10, 20 and 30 minutes after injection.

Successful sentinel lymph node (SLN) detection required at least one discrete fluorescent node on the intact mesocolon before mesenteric dissection. Candidate SLNs were marked, retrieved after specimen extraction, confirmed ex vivo by fluorescence and submitted separately for pathology (Fig. 2). Lymphatic mapping was recorded when fluorescent channels or basins were visible, irrespective of whether a discrete SLN was identified. Fluorescence did not alter the planned oncological extent of resection, and neither dose titration nor repeat injection was used.

Pathology, outcomes and statistics

All lymph nodes underwent routine haematoxylin and eosin assessment. The study record did not prospectively capture the grossing, embedding and sectioning details for non-sentinel nodes. Separately submitted sentinel nodes were processed individually: small nodes were bisected along the long axis, larger nodes were cut into 2-mm slices, and all tissue was embedded. Two or three haematoxylin and eosin sections were examined from each paraffin block alongside the whole case. A sentinel node containing metastasis on these sections was classified as positive without further work-up. If these sections were negative, a standardised departmental protocol used pan-cytokeratin

immunohistochemistry (CK AE1/AE3 ready-to-use antibody, Ventana/Roche), immediately followed by a haematoxylin and eosin section, at two levels 500 µm apart. Deposits were classified as isolated tumour cells, micrometastasis or macrometastasis according to the Union for International Cancer Control (UICC) tumour–node–metastasis (TNM) classification, 8th edition. A deposit at the lower end of the micrometastasis range could fall between the two examined levels. Isolated tumour cells remained pN0(i+) and were not counted as pN-positive, consistent with the American Joint Committee on Cancer (AJCC) 8th edition [32]. Ultrastaging was applied to sentinel nodes only. Non-sentinel nodes were examined by routine haematoxylin and eosin, as is standard in sentinel-node studies.

Reporting pathologists were not formally blinded to CT, intraoperative lymphadenopathy or sentinel designation. Treatment recommendations were sought in postoperative oncology records and, where available, multidisciplinary-team records.

Final composite pN combined routine non-sentinel-node histopathology with protocolised ultrastaging of ICG-selected sentinel nodes and served as the reference classification. Patient-level sensitivity, specificity, positive predictive value (PPV) and negative predictive value (NPV) for CT-LAP, CT-MTS and intraoperative lymphadenopathy were calculated among 38 invasive tumours. Specificity was calculated for these three clinical variables only and not for ICG-SLNB. The two pTis tumours remained in the cohort description but were excluded from invasive diagnostic and MMR-stratified analyses. Table 1 describes all 40 patients except where its legend states otherwise. Tables 2 and 3 describe the 38 invasive tumours. Table 4 separates 40 attempted procedures, 38 invasive tumours and 36 evaluable tumours with successful SLN detection. For ICG-SLNB, sensitivity and NPV were estimated among invasive tumours with successful SLN detection. SLN non-detection was reported separately as a technical procedural outcome and was not classified as a false-negative SLN result. The reference standard incorporated ultrastaging of the sentinel nodes themselves, so sentinel-node sensitivity and NPV were not independent of the index test (incorporation bias), and sentinel and non-sentinel nodes underwent different work-up (differential verification). An ultrastaging-detected deposit could be found only in a node that ICG-SLNB had already selected.

Fisher exact tests and Cohen kappa were used exploratorily. No confirmatory inference was planned. All hypothesis tests and p values are exploratory and carry no confirmatory error-rate guarantee. A descriptive post hoc Bonferroni analysis grouped four selected MMR comparisons: CT-LAP, CT-MTS, intraoperative lymphadenopathy and their CT-MTS-or-intraoperative composite. This family does not include every test reported in the manuscript, and the composite is derived from two components. It therefore does not provide manuscript-wide multiplicity control. No multivariable pN model was fitted because only 13 pN-positive events were available. For the MMR–CT-LAP association, the limiting features were n = 38, quasi-complete separation, sparse covariate overlap and collinearity rather than the pN event count. The study did not define a causal estimand or estimate an MMR effect independent of tumour phenotype.

Proportion confidence intervals used the Wilson method, and differences between independent proportions used the Newcombe hybrid score method without continuity correction. The paired comparison of CT-MTS with intraoperative lymphadenopathy was based on the exact binomial test of discordant correct classifications. The two variables were not assessed independently, because the operating surgeons knew the CT findings, so the discordance on which the test rests was probably reduced. The discrete bootstrap difference in kappa was retained in Additional file 1 only and was not used for null-hypothesis inference. Software versions, random seeds and bootstrap settings are reported in Additional file 1. Missing data were not imputed. All diagnostic-performance, specificity, restriction, multiplicity, kappa and paired analyses were post hoc, and the tumour-size restriction used a data-dependent cut-point taken from the cohort's own median.

OpenAI Codex and Anthropic Claude were used for language editing, consistency checks, preparation of revision suggestions and arithmetic cross-checks based on aggregate counts reported in the manuscript. They were not used to create or alter source patient data. Responsibility for the final analyses, interpretations and text rests with the authors.

Results

Cohort and MMR distribution

Forty patients were included (Fig. 1, Table 1). Most tumours were right-sided or proximal (29/40, 72.5%) and pT3–pT4 (28/40, 70.0%). pN-positive disease occurred in 13/40 patients (32.5%), and the median total lymph-node yield was 19 per patient (interquartile range [IQR] 15–24.3). One patient who met the cM0 entry criterion was upstaged at final pathology to pM1a (hepatic). This patient had dMMR, pT3 pN1b disease and a sentinel detection failure. All other patients were pM0.

MMR status was available for 38/40 patients: 14 dMMR and 24 pMMR. dMMR tumours were predominantly right-sided or proximal (13/14 vs 14/24). pN-positive disease occurred in 7/14 dMMR and 6/24 pMMR patients (difference + 25.0 percentage points, 95% CI − 5.6 to + 51.6; exploratory Fisher p = 0.16). The cohort did not resolve the direction or magnitude of this difference and does not establish equivalence. Individual MMR-protein loss patterns and MLH1 methylation results were not retained in the analysis extract, so the dMMR group could not be subdivided into sporadic and suspected hereditary categories. Table 1 summarises the cohort.

The 103 C18-coded resections that did not undergo the protocol form a descriptive institutional series rather than an eligible non-enrolled comparison. Within that series, 64/103 (62.1%) tumours were right-sided or proximal versus 29/40 (72.5%) in the analysed cohort (difference + 10.4 points, 95% CI − 7.3 to + 25.3). MMR was available for 89/103, including 27 dMMR tumours; with 14 missing results, the dMMR fraction among the 103 could range from 26.2% to 39.8%, so its direction relative to 14/38 (36.8%) in the analysed cohort is not fixed. Severity variables were unavailable, so these benchmarks do not resolve selection bias.

Table 1
Cohort characteristics and patient-level clinical nodal findings by postoperative MMR status.

Characteristic	Overall (n = 40)	dMMR (n = 14)	pMMR (n = 24)
Age, mean ± SD (years)	67.3 ± 11.8	68.9 ± 12.8	66.5 ± 11.5
BMI, mean ± SD (kg/m2)	27.8 ± 4.9	27.7 ± 4.2	27.8 ± 5.4
Male sex	22 (55.0%)	5 (35.7%)	16 (66.7%)
Open/robotic approach	23/17	10/4	12/12
Right/proximal tumour	29 (72.5%)	13 (92.9%)	14 (58.3%)
Largest tumour dimension, median (IQR), range (mm)	40 (30–61), 12–110	70 (44–79), 25–110	35 (25–41), 12–80
High-grade (G3) tumour	8/38 (21.1%)	7/14 (50.0%)	1/24 (4.2%)
pT3–pT4 disease	28 (70.0%)	12 (85.7%)	16 (66.7%)
Final pN-positive disease	13 (32.5%)	7 (50.0%)	6 (25.0%)
Lymphovascular invasion	10 (25.0%)	6 (42.9%)	4 (16.7%)
Total lymph node yield, median (IQR), range	19 (15–24.3), 7–42	20.5 (19.0–24.0), 12–42	17.5 (15.0–25.3), 7–37
Separately examined SLNs, median (IQR), range	2 (1–3), 1–9	2 (1–4), 1–9	2 (1–2.5), 1–6
CT-LAP ≥ 5-mm nodal-enlargement marker	21 (52.5%)	14 (100%)	7 (29.2%)
Study-defined CT-MTS composite	8 (20.0%)	6 (42.9%)	2 (8.3%)
Intraoperative lymphadenopathy	10 (25.0%)	7 (50.0%)	3 (12.5%)

Values are n (%) unless otherwise stated. Variables were complete for all 40 patients except MMR status (38/40). Two MMR-unknown patients (pTis cases) are included in the Overall column only. Separately examined SLNs are counted among the 36 invasive tumours with successful SLN detection. Because the pN-positive detection failure was dMMR and the pN-negative detection failure was pMMR, the stratum denominators for this row are 13 dMMR and 23 pMMR rather than the column-header denominators. Grade follows the World Health Organization (WHO) two-tier system, in which low grade comprises G1 and G2 and high grade comprises G3. The grade row excludes the two pTis patients, in whom no invasive carcinoma exists to grade, so its Overall denominator is 38. Quartiles were obtained by linear interpolation (equivalent to R type 7). Descriptively, dMMR tumours were larger and more often high grade. The count-based grade contrast had an exploratory Fisher p = 0.002. BMI, body mass index; IQR, interquartile range; SD, standard deviation.

CT-LAP, study-defined presence of at least one regional node with short-axis diameter ≥ 5 mm; CT-MTS, study-defined size-and-morphology CT suspicion composite; dMMR, mismatch-repair deficient; MMR, mismatch repair; pMMR, mismatch-repair proficient; SLN, sentinel lymph node.

Clinical nodal findings stratified by MMR status

CT-LAP was present in 14/14 dMMR and 7/24 pMMR tumours (difference + 70.8 points, 95% CI 41.4 to 85.1; exploratory Fisher p < 0.0001). Selected post hoc restrictions showed the same pattern. CT-LAP was present in 13/13 versus 6/14 right-sided or proximal tumours and 12/12 versus 6/16 pT3–pT4 tumours (Additional file 1, Table S1). Because every dMMR patient was CT-LAP-positive in the unrestricted analysis, 100% positivity within dMMR subsets is mathematically expected. A descriptive binomial bound on this universal positivity is reported in Additional file 1.

Post hoc grade and size restrictions produced the same directional pattern. CT-LAP occurred in 7/7 low-grade dMMR versus 7/23 low-grade pMMR tumours (difference + 69.6 points, 95% CI 28.7 to 84.4). Among tumours no larger than the data-derived cohort median of 40 mm, the corresponding counts were 4/4 versus 3/18 (difference + 83.3 points, 95% CI 29.4 to 94.2). Complementary estimates were 7/7 versus 0/1 for high-grade tumours and 10/10 versus 4/6 for tumours > 40 mm. Within pMMR tumours, CT-LAP occurred in 4/6 tumours > 40 mm and 3/18 tumours ≤ 40 mm (difference + 50.0 points, 95% CI 7.0 to 76.0). Additional file 1, Table S2 reports all differences and confidence intervals. The ≤ 40-mm restriction rests on four dMMR patients (Wilson 95% CI for 4/4, 51.0 to 100.0) and is therefore uninformative rather than confirmatory. These data-derived cuts do not isolate an MMR effect.

Between-group separation was smaller for the study-defined CT-MTS composite (6/14 vs 2/24; exploratory p = 0.034) and intraoperative lymphadenopathy (7/14 vs 3/24; exploratory p = 0.021). In the selected four-comparison Bonferroni sensitivity analysis, CT-LAP was the only individual comparison below the nominal 0.0125 threshold. The derived CT-MTS-or-intraoperative composite was also below this threshold. Because the family was selected post hoc, excludes other tests and contains a dependent composite, these results provide no confirmatory multiplicity guarantee (Additional file 1, Table S3).

The higher observed pN-positive proportion in dMMR tumours was imprecise (7/14 vs 6/24; difference + 25.0 points, 95% CI − 5.6 to + 51.6). Within the 14 dMMR patients, CT-MTS classified 9/14 correctly and intraoperative lymphadenopathy classified 12/14 correctly. Three patients were classified correctly only by intraoperative lymphadenopathy and none only by CT-MTS. The two-sided exact paired p value was 0.25. With three discordant pairs, 0.25 was the smallest two-sided value the test could return. This post hoc, non-independent comparison does not establish superiority. Kappa estimates and the joint patient table are reported descriptively in Additional file 1, Table S4.

Against final composite pN, CT-LAP was sensitive but non-specific, whereas CT-MTS and intraoperative lymphadenopathy each had 92.0% specificity (Table 2). CT-LAP specificity was 0/7 in dMMR and 15/18 in pMMR tumours (difference − 83.3 points, 95% CI − 94.2 to − 41.3; post hoc). Intraoperative

lymphadenopathy specificity was 6/7 in dMMR and 17/18 in pMMR tumours (difference − 8.7 points, 95% CI − 46.0 to + 14.6). These are patient-level, unadjusted and protocol-specific estimates. They neither identify the metastatic status of individual nodes nor isolate an MMR contribution.

Table 2
Patient-level clinical nodal classifications against final composite pN (n = 38).

Patient-level classification	TP/FP/FN/TN	Sensitivity	Specificity	PPV	NPV
CT-LAP ≥ 5-mm marker	11/10/2/15	84.6% (57.8–95.7)	60.0% (40.7–76.6)	52.4% (32.4–71.7)	88.2% (65.7–96.7)
Study-defined CT-MTS composite	6/2/7/23	46.2% (23.2–70.9)	92.0% (75.0–97.8)	75.0% (40.9–92.9)	76.7% (59.1–88.2)
Intraoperative lymphadenopathy	8/2/5/23	61.5% (35.5–82.3)	92.0% (75.0–97.8)	80.0% (49.0–94.3)	82.1% (64.4–92.1)

Point estimates are accompanied by Wilson 95% confidence intervals. CT-LAP is shown as an analytical positive classification to quantify its relationship with pN. It was not intended as a clinical metastatic threshold. Fisher association p values were omitted because they do not test acceptable diagnostic performance. No prespecified sensitivity or specificity target was available, and no multivariable model was fitted.

CT-LAP, study-defined ≥ 5-mm CT nodal-enlargement marker; CT-MTS, study-defined size-and-morphology CT suspicion composite; FN, false negative; FP, false positive; NPV, negative predictive value; PPV, positive predictive value; TN, true negative; TP, true positive.

ICG-SLNB performance and sentinel-node ultrastaging

SLNs were detected in 38/40 patients (95.0%, 95% CI 83.5 to 98.6) and in 36/38 invasive tumours (94.7%). The 36 invasive tumours with successful SLN detection had a median of 2 SLNs per patient (IQR 1–3). Detection occurred in 22/23 open procedures (95.7%) and 16/17 robotic procedures (94.1%). Lymphatic mapping succeeded in 34/40 patients, and fluorescence altered the perceived operative field or dissection plan in 9/40 patients. The planned oncological extent of resection was unchanged in all of them. In five patients with detection but no mapping, discrete fluorescent nodes were visible without identifiable lymphatic channels. Because mapped compartments were not separately labelled for pathology, this remained an anatomical observation.

Two procedures had no detected sentinel node: one pN-negative pMMR patient and one pN-positive dMMR patient. Among the 12 pN-positive patients with successful SLN detection, six had a positive sentinel node and six had a false-negative SLN result. Sensitivity was 50.0% (6/12, 95% CI 25.4 to 74.6), and NPV was 80.0% (24/30, 95% CI 62.7 to 90.5). The pN-positive non-detection was reported as a

technical failure and was not included in the sensitivity denominator. Treating that procedure as a failure to identify nodal disease, the intention-to-diagnose sensitivity was 46.2% (6/13, 95% CI 23.2 to 70.9).

Six procedures with a detected sentinel node were false negative. Four patients had a single positive node, all pN1a macrometastases. The other two had pN1b and pN2b disease. The additional pN-positive non-detection occurred in a dMMR patient with pN1b disease. Among the six false-negative SLN results after successful SLN detection, the number of separately examined sentinel nodes had a median of 2 (range 1–6), compared with 1 (range 1–2) among six true positives. These small post hoc groups cannot distinguish procedural under-sampling, tracer-flow failure, disease spectrum or MMR-associated heterogeneity. Among the six true positives, one patient had pN1a, four had pN1b and one had pN2b disease.

Ultrastaging identified isolated tumour cells in six patients. Four otherwise pN0 patients were reclassified as pN0(i+), and two pN-positive patients had additional isolated tumour cells. No micrometastasis or pN0-to-pN-positive upstaging was observed. For zero upstagings among the 24 pN-negative patients with successful SLN detection, the upper limit of the two-sided 95% Wilson interval was 13.8%. The available record did not define a complete denominator for treatment recommendations. It also did not define a prospective method or time window for adverse-event ascertainment. No immediate hypersensitivity reaction or other adverse event attributable to indocyanine green was recorded in the operative or discharge records. Treatment impact, clinical benefit and a protocol-defined safety outcome were therefore not assessed.

Of 145 C18-coded colonic resections identified in the administrative log during the study period, 42 underwent the ICG-SLNB protocol. After two post-enrolment exclusions, 40 attempts remained. Of these, 38 were invasive tumours and 36 had detected sentinel nodes. The inset 2×2 table includes procedures with successful detection only (TP 6, FP 0, FN 6, TN 24).

Table 3
MMR-stratified patient-level clinical nodal classifications against final composite pN.

Patient-level classification	MMR status	TP/FP/FN/TN	Sensitivity	Specificity
CT-LAP ≥ 5-mm marker	dMMR	7/7/0/0	7/7 (100%, 64.6–100.0)	0/7 (0%, 0.0–35.4)
CT-LAP ≥ 5-mm marker	pMMR	4/3/2/15	4/6 (66.7%, 30.0–90.3)	15/18 (83.3%, 60.8–94.2)
Study-defined CT-MTS composite	dMMR	4/2/3/5	4/7 (57.1%, 25.0–84.2)	5/7 (71.4%, 35.9–91.8)
Study-defined CT-MTS composite	pMMR	2/0/4/18	2/6 (33.3%, 9.7–70.0)	18/18 (100%, 82.4–100.0)
Intraoperative lymphadenopathy	dMMR	6/1/1/6	6/7 (85.7%, 48.7–97.4)	6/7 (85.7%, 48.7–97.4)
Intraoperative lymphadenopathy	pMMR	2/1/4/17	2/6 (33.3%, 9.7–70.0)	17/18 (94.4%, 74.2–99.0)

CT-LAP flagged every dMMR patient. Its dMMR sensitivity of 7/7 and specificity of 0/7 are therefore restatements of universal positivity, not independent evidence of discrimination. The criterion was a binary ≥ 5-mm enlargement marker rather than a validated metastasis rule. The between-stratum specificity contrast is descriptive and post hoc. Small within-stratum cells preclude transportable estimates or inference about an independent MMR effect.

For CT-LAP, the post hoc between-stratum specificity difference (dMMR minus pMMR) was − 83.3 percentage points (95% CI − 94.2 to − 41.3).

CT-LAP, study-defined ≥ 5-mm CT nodal-enlargement marker; CT-MTS, study-defined size-and-morphology CT suspicion composite; dMMR, mismatch-repair deficient; FN, false negative; FP, false positive; MMR, mismatch repair; pMMR, mismatch-repair proficient; pN, pathological nodal status; TN, true negative; TP, true positive.

Table 4
ICG-SLNB detection and sensitivity after successful SLN detection against final composite pN.

Outcome	n	Definition / interpretation
Cohort	40	All analysed attempted procedures after two post-enrolment exclusions
SLN detection	38/40 (95.0%, 95% CI 83.5–98.6)	At least one discrete fluorescent SLN identified
Separately examined SLNs	82 in 36 evaluable cases	Median 2 (IQR 1–3, range 1–9)
Lymphatic mapping success	34/40 (85.0%)	Fluorescent channels and/or basins visible; anatomical outcome
Invasive tumours	38	Two pTis tumours excluded from invasive diagnostic estimates
SLN-evaluable invasive tumours	36/38	Invasive tumour, detected SLN and protocol-compliant SLN pathology
True-positive SLNB	6	SLN-positive in a pN-positive patient
True-negative SLNB	24	SLN-negative in a pN-negative patient under final composite pN
False-negative SLNB after successful detection	6	SLN-negative in a pN-positive patient (4 dMMR, 2 pMMR)
False-positive SLNB	0	Structurally impossible because SLN metastasis contributes to final composite pN
No SLN detected	2	One pN-negative pMMR and one pN-positive dMMR procedure; reported as technical non-detection
SLN sensitivity after successful detection	50.0% (6/12, 95% CI 25.4–74.6)	TP / (TP + FN) among pN-positive patients with detected SLNs
NPV after successful detection	80.0% (24/30, 95% CI 62.7–90.5)	TN / (TN + FN) among procedures with detected SLNs
False-negative rate after successful detection	50.0% (6/12)	Complement of sensitivity; non-detection is not classified as false negative
Ultrastaging yield	ITC in 6; pN-positive upstaging 0/24	No micrometastasis; upper limit of two-sided 95% Wilson CI for upstaging 13.8%

The 2×2 table (TP 6, FP 0, FN 6, TN 24) includes procedures with successful SLN detection only. The pN-positive non-detection was reported separately as a technical failure and not classified as a false-negative SLN result. Isolated tumour cells remained pN0(i+) and were not counted as SLN-positive or pN-positive. Final composite pN rested on routine histopathology of all harvested nodes, with

protocolised ultrastaging applied to haematoxylin and eosin-negative ICG-selected sentinel nodes. Ultrastaging could also have upstaged a routinely negative case through micrometastasis, which may make sensitivity after successful SLN detection and NPV optimistic. No such upstaging occurred in this cohort, so the caveat is structural rather than an observed effect. Specificity and PPV are therefore not presented as independent diagnostic properties.

CI, confidence interval; FN, false negative; FP, false positive; ICG, indocyanine green; IQR, interquartile range; ITC, isolated tumour cells; NPV, negative predictive value; pN, pathological nodal status; SLN, sentinel lymph node; SLNB, sentinel lymph node biopsy; TN, true negative; TP, true positive.

(a–c) Robotic approach. (a) Subserosal peritumoural ICG injection. (b) Fluorescence-guided identification and clip marking of a sentinel lymph node (SLN). (c) Fluorescent SLN within the mesocolon.

(d–f) Open approach. (d) Suture marking of fluorescent SLNs. (e) Centrally located SLNs (yellow rings mark the fluorescent sentinel nodes). The blue arrow indicates the course of the superior mesenteric vein. (f) Fluorescent SLNs and lymphatic channels in a mesocolic location. ICG, indocyanine green; SLN, sentinel lymph node.

Discussion

To our knowledge, this is the first prospective cohort to report indocyanine green-guided sentinel-node mapping and a blinded retrospective CT nodal reread in the same patients, stratified by postoperative mismatch-repair status, the design proposed by Stratton et al. [26]. We identified no prior cohort combining both assessments within MMR strata. The three nodal assessments addressed different constructs and are not a head-to-head comparison. Together they produced a dissociation. A deliberately sensitive enlargement marker was positive in every dMMR patient yet separated no dMMR patient from another by pN status, while a tracer that found sentinel nodes in almost every procedure captured only half of the pN-positive disease it was applied to.

The CT finding should be read within the co-distributed dMMR and right-sided phenotype rather than attributed to MMR alone. This study examined neither the histology of enlarged non-metastatic nodes nor any means of separating immune-reactive enlargement from tumour size, location, grade or measurement effects. Platt et al. reported that, among cases with an incorrectly classified N status, 90% of dMMR and 59% of pMMR were overstaged [8], and a series of 78 dMMR colon cancers reported 55% nodal-stage accuracy [15]. Reactive inflammatory lymphadenopathy is biologically consistent with the immune-rich dMMR phenotype [8, 11, 12], and stage-adjusted nodal metastasis has been lower than in pMMR disease [14]. Nodal size is in any case a weak discriminator. More than half of metastatic nodes measure 5 mm or less, and right-sided tumours contain larger metastatic and benign nodes alike [9]. A station-level study found that the ratio of CT-suspicious to histologically positive nodes ranged from 0.92 at central to 5.30 at intermediate nodal stations [29], and a meta-analysis of 44 studies pooled CT specificity at 67% [33]. Rollvén et al. found no reliable size threshold [10], a recent series omitted size

from its high-risk criteria [34], and Node-RADS assigns only low suspicion to enlargement without abnormal configuration [30]. NICHE-2 assumed rather than measured overstaging in approximately one-quarter of clinically node-positive dMMR patients [7]. These contextualise but do not replicate the present ≥ 5-mm marker, and the observed pN difference was too imprecise to separate sampling variation or cohort composition from a spectrum-specific difference.

ICG-SLNB showed a different limitation. Reliable detection did not ensure procedural capture of metastatic disease. The 95.0% detection rate is consistent with pooled estimates of 91–94% and sits within the broader published range, which includes a 72.6% colorectal subgroup rate in EURO-FIGS and a 55–100% range in a colon-only review [21, 23, 24, 35]. Sensitivity after successful SLN detection was 50.0%, below pooled values of 63–71% and close to a prospective report of 44% [21, 24, 36]. These cross-study comparisons are descriptive, because injection protocols, detection rules, non-detection handling and reference pathways differ [25]. The asymmetric node-level work-up here, in which sentinel ultrastaging could itself alter pN, also prevents interpretation as an unbiased intrinsic test property.

Several mechanisms could explain a tumour-bearing node that fluorescence did not flag. Fluorescence traces lymphatic flow rather than tumour content. Sato et al. found metastases more often in fluorescence-negative nodes and loss of signal when tumour replaced most of a node [22], as did Kakizoe et al. in completely replaced nodes [37]. Drainage may not be stepwise [38, 39], injection timing changes the number of traced nodes [40], and in vivo and ex vivo mapping identify different node sets [41]. Disease spectrum and technique are equally likely explanations. Sentinel sensitivity is lower in T3–T4 than T1–T2 disease [42] and this cohort was predominantly pT3–pT4, while injection depth, operator learning, two fluorescence platforms and the open-versus-robotic workflow varied across procedures. Multicentre blue-dye trials reported similarly high false-negative rates [16, 17]. The six false-negative results after successful detection and the single pN-positive non-detection may have different causes, which this study cannot distinguish.

A biological link between MMR status, CT enlargement and tracer behaviour remains a hypothesis. Inamori et al. found greater tumour-to-node T-cell receptor overlap in dMMR than pMMR disease [43], and reactive follicular and parafollicular hyperplasia can enlarge tumour-free nodes [44]. This study measured neither immune architecture nor the histology of enlarged pN-negative nodes.

Ultrastaging had limited observed yield: isolated tumour cells in six patients, no micrometastasis and no pN-positive upstaging. Because only two levels 500 µm apart were examined, this is the yield of the protocol rather than the prevalence of low-volume disease. The 13.8% upper confidence limit for zero upstagings among the 24 pN-negative patients with successful SLN detection addresses sampling variation but not deposits missed between levels. Pooled estimates of 2% sentinel-node and 6% non-sentinel-node upstaging arise from heterogeneous protocols [45], and isolated tumour cells should remain distinct from micrometastases, which carry different prognostic evidence [3, 21]. More sensitive assays increase detection without resolving clinical significance. Bilchik et al. found occult disease in 16/30 sentinel-negative patients using immunohistochemistry and reverse-transcription PCR [19].

Nordgård et al. found frequent molecular positivity without a prognostic effect [20], and Hirche et al. assigned chemotherapy to three patients with sentinel-node isolated tumour cells [46]. A review nevertheless still regards the clinical value of low-volume disease as unestablished [18]. Directing postoperative pathology is one potential application, but it was not validated here as no selection rule was tested and non-sentinel nodes were not ultrastaged symmetrically.

Intraoperative lymphadenopathy classified 12/14 dMMR patients correctly compared with 9/14 for CT-MTS, but the exact paired comparison rested on three versus zero discordances ($p = 0.25$) and does not establish superiority. The corresponding dMMR-versus-pMMR comparisons for CT-MTS and intraoperative lymphadenopathy do not themselves survive the four-comparison correction reported in Additional file 1, Table S3. Surgeons knew the CT findings, applied no fixed criterion and used different sensory information in open and robotic procedures.

Prior studies show that most metastases lie within the tumour-bearing segment and that some central-node metastases escape CT suspicion [47, 48]. They do not, however, validate this variable, which would require a prespecified, blinded and independently adjudicated comparison.

Read together, these findings indicate that a ≥ 5-mm nodal threshold cannot be used to infer metastatic risk in dMMR tumours of this phenotype, which were predominantly right-sided, large and pT3–pT4. Whether size-independent morphology performs better is untested here, because the study-defined CT-MTS composite was only 46.2% sensitive. Internal heterogeneity nevertheless discriminated well in the colon cohort of Rollvén et al. (odds ratio 20.0; 79% sensitivity, 84% specificity) [10] and warrants prospective evaluation in MMR-stratified disease. Because MMR status was determined postoperatively, this cohort cannot address whether preoperatively known MMR status should alter radiological reporting. The sentinel findings separately indicate that feasible detection does not make SLNB a standalone staging tool outside a trial, and that its role in directing focused pathology remains hypothetical.

Selection and sample size set the main inferential ceiling. The cohort was single-centre, availability-based and non-consecutive, with 13 pN-positive events and seven pN-negative dMMR patients supporting the headline specificity. The 103 non-protocol C18-coded resections could not serve as an eligible non-enrolled comparison. The administrative log lacked the biopsy, elective-status and exclusion-criterion fields needed to reconstruct eligibility, and the benchmark extract lacked pT, pN, tumour size, age, sex and operative approach. Eligible non-enrolled patients were not recorded prospectively. Selection and spectrum bias therefore remain unresolved, and prevalence-dependent PPV and NPV cannot be transported. MMR was postoperative and co-distributed with sidedness, size and grade, with further imbalances in pT, lymphovascular invasion, operative approach and node yield. Median tumour size was 70 mm in dMMR and 35 mm in pMMR tumours, so tumour burden is a sufficient alternative explanation for both the CT-LAP gradient and the pN difference. Nodal yield had a median of 20.5 in the dMMR stratum and 17.5 in the pMMR stratum, with overlapping interquartile ranges and no test of interaction. This distribution could raise pN-positive ascertainment and therefore makes the stratum

difference in pN partly dependent on the pathology pathway itself. One-variable post hoc restrictions are not independent replications and do not control these joint distributions.

Measurement limitations further constrain each modality. CT used a single reader without a reliability estimate, which should be read against published interrater agreement of κ 0.63 for CT nodal staging in dMMR colon cancer (0.60 to 0.64 across stage categories) [15], and CT-MTS gated incompletely specified morphology behind size. The acquisition, interval and reader-access parameters listed in the Methods, together with PET/CT type, were not documented in the study materials. A longer CT-to-resection interval would generally favour understaging and is unlikely by itself to explain the dMMR CT-LAP pattern, but its effect cannot be measured here. Intraoperative lymphadenopathy combined CT-aware operative judgement with approach-dependent sensory information and specimen examination, and final composite pN was established without formal blinding. The study did not measure recurrence, survival or clinical benefit, and the analysis extract did not identify a complete assessable denominator, so treatment impact was not analysed. Given the absence of registration and of a timestamped protocol or analysis plan noted in the Methods, no causal, confirmatory or practice-changing inference is warranted.

Fluorescence mapping may have an anatomical role this study was not designed to establish. It altered the perceived operative field or dissection plan in nine patients without changing the planned extent of resection, and mapped compartments were not separately labelled for pathological validation. Other studies report concordance between fluorescent drainage and metastatic-node location, though prespecified performance targets have not been met consistently [49, 50]. Future work should keep three questions apart: whether fluorescence identifies a valid sentinel node, improves pathological sampling or guides resection. Validation requires consecutive recruitment with a screening log, preoperative MMR testing (feasible from biopsy specimens given quality safeguards [5, 6]) and enough left-sided dMMR tumours to separate MMR-associated patterns from sidedness. Protocols should prespecify the estimand, performance and precision targets and the handling of non-detection and multiplicity. Imaging should use multiple blinded readers and colon-specific descriptors based on configuration and distribution [30]. Sentinel studies should use symmetric work-up of sentinel and non-sentinel nodes with recurrence follow-up, against the pericolic and central spread benchmarks of the T-REX study [51].

Conclusions

In this selected, availability-based, non-consecutive cohort, all 14 dMMR patients had at least one regional node measuring ≥ 5 mm on blinded retrospective CT reread. Within the dMMR stratum, that marker did not separate pN-positive from pN-negative disease. The study-defined CT-MTS composite was more specific and only 46.2% sensitive. Neither CT variable was validated as a stand-alone staging rule.

ICG-SLNB detected sentinel nodes in 38/40 procedures, yet among 12 pN-positive patients with successful SLN detection sensitivity was 6/12, with one further pN-positive dMMR procedure ending in

non-detection. These estimates arose under an asymmetric pathology pathway in which ICG-selected nodes were assessed more intensively and contributed to the reference standard. Two-level ultrastaging produced no upstaging, though a non-zero yield cannot be excluded.

MMR status was postoperative and co-distributed with sidedness, tumour size and grade. This cohort cannot establish an independent MMR effect, comparative superiority or transportable accuracy. Consecutive, prespecified, preoperatively MMR-stratified validation with symmetric pathology and clinically relevant follow-up is required.

Abbreviations

AJCC
American Joint Committee on Cancer
BMI
body mass index
CI
confidence interval
CT
computed tomography
CT-LAP
study-defined ≥ 5-mm CT nodal-enlargement marker
CT-MTS
study-defined size-and-morphology CT suspicion composite
dMMR
mismatch-repair deficient
FN
false negative
FP
false positive
ICG
indocyanine green
ICG-SLNB
indocyanine green-guided sentinel lymph node biopsy
IQR
interquartile range
ITC
isolated tumour cells
MMR
mismatch repair
MRI
magnetic resonance imaging

Node-RADS
Node Reporting and Data System
NPV
negative predictive value
PCR
polymerase chain reaction
PET/CT
positron emission tomography/computed tomography
pMMR
mismatch-repair proficient
pN
pathological nodal status
PPV
positive predictive value
SD
standard deviation
SLN
sentinel lymph node
SLNB
sentinel lymph node biopsy
STARD
Standards for Reporting of Diagnostic Accuracy Studies
STROBE
Strengthening the Reporting of Observational Studies in Epidemiology
TN
true negative
TNM
tumour–node–metastasis
TP
true positive
UICC
Union for International Cancer Control
WHO
World Health Organization.

Declarations

Ethics approval and consent to participate

The study was approved by the institutional Ethics Committee of Masaryk Memorial Cancer Institute (ref. 2024/1287/MOU, 7 May 2024). All participants provided written informed consent. The study was

not entered in a public trials registry. It was designed as a prospective observational cohort evaluating an intraoperative imaging adjunct. Fluorescence findings did not determine the planned oncological extent of resection, and no health outcome was assigned as an intervention endpoint.

Consent for publication

Not applicable. The intraoperative photographs in Fig. 2 contain no identifiable individual patient features, and no identifiable individual patient data are reported. Consent for publication was therefore not required.

Competing interests

The authors declare that they have no competing interests.

Use of artificial intelligence tools

As described in the Methods, large language model tools (OpenAI Codex and Anthropic Claude) were used for language editing, consistency checks, preparation of revision suggestions and arithmetic cross-checks based on aggregate counts reported in the manuscript. They were not used to create or alter source patient data. Responsibility for the final analyses, interpretations and text rests with the authors.

Funding

This research received no specific grant from any funding agency in the public, commercial or not-for-profit sectors.

Author Contribution

T.S. conceived and designed the study, contributed to the investigation, validation and formal analysis, and wrote the original draft. Z.M. contributed to the conception, design and methodology and to writing the original draft. L.F. contributed to the investigation. S.J. contributed to the investigation and the formal analysis. V.F. contributed to the conception, design, methodology and validation. All authors reviewed and approved the final manuscript.

Acknowledgements

Not applicable.

Data Availability

De-identified data and analysis code are available from the corresponding author on reasonable request. Unrestricted public deposition is precluded because patient-level data from this small cohort carry a residual re-identification risk, and sharing is subject to institutional and ethical approval. The study protocol approved by the institutional Ethics Committee (ref. 2024/1287/MOU) is likewise available on request. It was not deposited in a public registry or repository before enrolment.

References

1. Argilés G, Tabernero J, Labianca R, Hochhauser D, Salazar R, Iveson T, et al. Localised colon cancer: ESMO Clinical Practice Guidelines for diagnosis, treatment and follow-up. Ann Oncol. 2020;31:1291–305. https://doi.org/10.1016/j.annonc.2020.06.022.
2. Bertelsen CA, Kirkegaard-Klitbo A, Nielsen M, Leotta SM, Fukumori D, Gögenur I. Pattern of colon cancer lymph node metastases in patients undergoing central mesocolic lymph node excision: a systematic review. Dis Colon Rectum. 2016;59:1209–21. https://doi.org/10.1097/DCR.0000000000000658.
3. Sloothaak DAM, Sahami S, van der Zaag-Loonen HJ, van der Zaag ES, Tanis PJ, Bemelman WA, et al. The prognostic value of micrometastases and isolated tumour cells in histologically negative lymph nodes of patients with colorectal cancer: a systematic review and meta-analysis. Eur J Surg Oncol. 2014;40:263–9. https://doi.org/10.1016/j.ejso.2013.12.002.
4. Vangala DB, Seufferlein T, Hüneburg R. Lynch syndrome in context of the updated German S3 guideline colorectal cancer: implementation of universal MMR/MSI testing. Oncol Res Treat. 2026;49:165–73. https://doi.org/10.1159/000547331.
5. Grillo F, Paudice M, Gambella A, Bozzano S, Sciallero S, Puccini A, et al. Evaluating mismatch repair deficiency in colorectal cancer biopsy specimens. Histochem Cell Biol. 2023;160:113–25. https://doi.org/10.1007/s00418-023-02202-8.
6. Vazzano J, Tomlinson J, Stanich PP, Pearlman R, Kalady MF, Chen W, et al. Universal tumor screening for Lynch syndrome on colorectal cancer biopsies impacts surgical treatment decisions. Fam Cancer. 2023;22:71–6. https://doi.org/10.1007/s10689-022-00302-3.
7. Chalabi M, Verschoor YL, Tan PB, Balduzzi S, Van Lent AU, Grootscholten C, et al. Neoadjuvant immunotherapy in locally advanced mismatch repair-deficient colon cancer. N Engl J Med. 2024;390:1949–58. https://doi.org/10.1056/NEJMoa2400634.
8. Platt JR, Ansett J, Seligmann JF, West NP, Tolan DJM. The impact of mismatch repair status and systemic inflammatory markers on radiological staging in colon cancer. Br J Radiol. 2023;96:20230098. https://doi.org/10.1259/bjr.20230098.
9. Yamaoka Y, Kinugasa Y, Shiomi A, Yamaguchi T, Kagawa H, Yamakawa Y, et al. The distribution of lymph node metastases and their size in colon cancer. Langenbecks Arch Surg. 2017;402:1213–21. https://doi.org/10.1007/s00423-017-1628-z.

10. Rollvén E, Abraham-Nordling M, Holm T, Blomqvist L. Assessment and diagnostic accuracy of lymph node status to predict stage III colon cancer using computed tomography. Cancer Imaging. 2017;17:3. https://doi.org/10.1186/s40644-016-0104-2.
11. Nowak M, Jabbar F, Rodewald A-K, Gneo L, Tomasevic T, Harkin A, et al. Single-cell AI-based detection and prognostic and predictive value of DNA mismatch repair deficiency in colorectal cancer. Cell Rep Med. 2024;5:101727. https://doi.org/10.1016/j.xcrm.2024.101727.
12. Becht E, de Reyniès A, Giraldo NA, Pilati C, Buttard B, Lacroix L, et al. Immune and stromal classification of colorectal cancer is associated with molecular subtypes and relevant for precision immunotherapy. Clin Cancer Res. 2016;22:4057–66. https://doi.org/10.1158/1078-0432.CCR-15-2879.
13. Belt EJ, te Velde EA, Krijgsman O, Brosens RP, Tijssen M, van Essen HF, et al. High lymph node yield is related to microsatellite instability in colon cancer. Ann Surg Oncol. 2012;19:1222–30. https://doi.org/10.1245/s10434-011-2091-7.
14. Hakki L, Khan A, Gonen M, Stadler Z, Segal NH, Shia J, et al. Lymph node metastases and associated recurrence-free survival in microsatellite stable and unstable colon cancer. Ann Surg Oncol. 2023;30:8487–94. https://doi.org/10.1245/s10434-023-14270-0.
15. Linhares SM, Srikumar T, Shin C, Mathur M, Alkukhun A, Mongiu AK et al. Accuracy of computed tomography staging of mismatch repair-deficient colon cancer. JCO Oncol Pract 2025 Nov 18:OP2500505. Epub ahead of print. https://doi.org/10.1200/OP-25-00505
16. Bertagnolli M, Miedema B, Redston M, Dowell J, Niedzwiecki D, Fleshman J, et al. Sentinel node staging of resectable colon cancer: results of a multicenter study. Ann Surg. 2004;240:624–30. https://doi.org/10.1097/01.sla.0000140753.41357.20.
17. Bembenek AE, Rosenberg R, Wagler E, Gretschel S, Sendler A, Siewert JR, et al. Sentinel lymph node biopsy in colon cancer: a prospective multicenter trial. Ann Surg. 2007;245:858–63. https://doi.org/10.1097/01.sla.0000250428.46656.7e.
18. Huynh KT, Bilchik AJ. Sentinel lymph node biopsy and nodal ultrastaging in colorectal cancer. Cancer J. 2015;21:11–6. https://doi.org/10.1097/PPO.0000000000000093.
19. Bilchik AJ, Saha S, Wiese D, Stonecypher JA, Wood TF, Sostrin S, et al. Molecular staging of early colon cancer on the basis of sentinel node analysis: a multicenter phase II trial. J Clin Oncol. 2001;19:1128–36. https://doi.org/10.1200/JCO.2001.19.4.1128.
20. Nordgård O, Oltedal S, Aasprong OG, Søreide JA, Søreide K, Tjensvoll K, et al. Prognostic relevance of occult metastases detected by cytokeratin 20 and mucin 2 mRNA levels in sentinel lymph nodes from colon cancer patients. Ann Surg Oncol. 2012;19:3719–26. https://doi.org/10.1245/s10434-012-2454-8.
21. Ankersmit M, Bonjer HJ, Hannink G, Schoonmade LJ, van der Pas MHGM, Meijerink WJHJ. Near-infrared fluorescence imaging for sentinel lymph node identification in colon cancer: a prospective single-center study and systematic review with meta-analysis. Tech Coloproctol. 2019;23:1113–26. https://doi.org/10.1007/s10151-019-02107-6.

22. Sato Y, Satoyoshi T, Okita K, Kyuno D, Hamabe A, Okuya K, et al. Snapshots of lymphatic pathways in colorectal cancer surgery using near-infrared fluorescence, in vivo and ex vivo. Eur J Surg Oncol. 2021;47:3130–6. https://doi.org/10.1016/j.ejso.2021.07.025.
23. Negrut RL, Cote A, Feder B, Bodog FD, Maghiar AM. Enhanced lymph node detection in colon cancer using indocyanine green fluorescence: a systematic review of studies from 2020 onwards. J Pers Med. 2025;15:54. https://doi.org/10.3390/jpm15020054.
24. Villegas-Tovar E, Jimenez-Lillo J, Jimenez-Valerio V, Diaz-Giron-Gidi A, Faes-Petersen R, Otero-Piñeiro A, et al. Performance of indocyanine green for sentinel lymph node mapping and lymph node metastasis in colorectal cancer: a diagnostic test accuracy meta-analysis. Surg Endosc. 2020;34:1035–47. https://doi.org/10.1007/s00464-019-07274-z.
25. Litchinko A, Meyer J, Buhler L, Ris F, Adamina M. Fluorescence indocyanine green (ICG) for sentinel-lymph-node mapping in colorectal cancer: a systematic review. Langenbecks Arch Surg. 2025;410:202. https://doi.org/10.1007/s00423-025-03786-6.
26. Stratton M, Davies J, Joshi H. Rethinking lymphadenectomy in the immunotherapy era of colorectal cancer: a hypothesis-generating perspective. Colorectal Dis. 2026;28:e70539. https://doi.org/10.1111/codi.70539.
27. von Elm E, Altman DG, Egger M, Pocock SJ, Gøtzsche PC, Vandenbroucke JP. The Strengthening the Reporting of Observational Studies in Epidemiology (STROBE) statement: guidelines for reporting observational studies. Lancet. 2007;370:1453–7. https://doi.org/10.1016/S0140-6736(07)61602-X.
28. Bossuyt PM, Reitsma JB, Bruns DE, Gatsonis CA, Glasziou PP, Irwig L, et al. STARD 2015: an updated list of essential items for reporting diagnostic accuracy studies. BMJ. 2015;351:h5527. https://doi.org/10.1136/bmj.h5527.
29. Simu P, Jung I, Banias L, Fulop ZZ, Bara T, Simu I, et al. In-house validated map of lymph node stations in a prospective cohort of colorectal cancer: a tool for a better preoperative staging. J Oncol. 2022;2022:1788004. https://doi.org/10.1155/2022/1788004.
30. Elsholtz FHJ, Asbach P, Haas M, Becker M, Beets-Tan RGH, Thoeny HC, et al. Introducing the Node Reporting and Data System 1.0 (Node-RADS): a concept for standardized assessment of lymph nodes in cancer. Eur Radiol. 2021;31:6116–24. https://doi.org/10.1007/s00330-020-07572-4.
31. Beets-Tan RGH, Lambregts DMJ, Maas M, Bipat S, Barbaro B, Curvo-Semedo L, et al. Magnetic resonance imaging for clinical management of rectal cancer: updated recommendations from the 2016 European Society of Gastrointestinal and Abdominal Radiology (ESGAR) consensus meeting. Eur Radiol. 2018;28:1465–75. https://doi.org/10.1007/s00330-017-5026-2.
32. Weiser MR. AJCC 8th edition: colorectal cancer. Ann Surg Oncol. 2018;25:1454–5. https://doi.org/10.1245/s10434-018-6462-1.
33. Shkurti J, van den Berg K, Tissier RLM, van der Mierden S, Lahaye MJ, Beets-Tan RGH, et al. Diagnostic accuracy of CT for identifying high-risk colon cancer: a systematic review and meta-analysis. Eur Radiol. 2026;36:1012–24. https://doi.org/10.1007/s00330-025-11844-2.

34. Son GM, Kim TU, Yun MS, Kim C, Lee IY, Park SB, et al. Effect of fluorescence lymph node mapping on improving diagnostic values of CT D3 lymph node staging for right-sided colon cancer. Cancers (Basel). 2024;16:3496. https://doi.org/10.3390/cancers16203496.
35. Picchetto A, Cinelli L, Bannone E, Baiocchi GL, Morales-Conde S, Casali L, et al. Fluorescence-based sentinel lymph node mapping and lymphography evaluation: results from the IHU-IRCAD-EAES EURO-FIGS registry. Surg Endosc. 2023;37:5472–81. https://doi.org/10.1007/s00464-023-10043-8.
36. Emile SH, Elfeki H, Shalaby M, Sakr A, Sileri P, Laurberg S, et al. Sensitivity and specificity of indocyanine green near-infrared fluorescence imaging in detection of metastatic lymph nodes in colorectal cancer: systematic review and meta-analysis. J Surg Oncol. 2017;116:730–40. https://doi.org/10.1002/jso.24701.
37. Kakizoe M, Watanabe J, Suwa Y, Nakagawa K, Suwa H, Ozawa M, et al. The histopathological evaluation based on the indocyanine green fluorescence imaging of regional lymph node metastasis of splenic flexural colon cancer by near-infrared observation. Int J Colorectal Dis. 2021;36:717–23. https://doi.org/10.1007/s00384-020-03798-2.
38. Zhang C, Zhang L, Xu T, Xue R, Yu L, Zhu Y, et al. Mapping the spreading routes of lymphatic metastases in human colorectal cancer. Nat Commun. 2020;11:1993. https://doi.org/10.1038/s41467-020-15886-6.
39. Chang C-Y, Lin C-C, Lin H-H, Lan Y-T, Chang S-C, Wang H-S, et al. The negative prognostic impact of lymph node skip metastasis in stage III colon cancer with pN1 disease: a single-center and retrospective cohort study. Dis Colon Rectum. 2023;66:e1032–42. https://doi.org/10.1097/DCR.0000000000002383.
40. Lucas K, Melling N, Giannou AD, Reeh M, Mann O, Hackert T, et al. Lymphatic mapping in colon cancer depending on injection time and tracing agent: a systematic review and meta-analysis of prospective designed studies. Cancers (Basel). 2023;15:3196. https://doi.org/10.3390/cancers15123196.
41. Andersen HS, Bennedsen ALB, Burgdorf SK, Eriksen JR, Eiholm S, Toxværd A, et al. In vivo and ex vivo sentinel node mapping does not identify the same lymph nodes in colon cancer. Int J Colorectal Dis. 2017;32:983–90. https://doi.org/10.1007/s00384-017-2777-9.
42. Burghgraef TA, Zweep AL, Sikkenk DJ, van der Pas MHGM, Verheijen PM, Consten ECJ. In vivo sentinel lymph node identification using fluorescent tracer imaging in colon cancer: a systematic review and meta-analysis. Crit Rev Oncol Hematol. 2021;158:103149. https://doi.org/10.1016/j.critrevonc.2020.103149.
43. Inamori K, Togashi Y, Fukuoka S, Akagi K, Ogasawara K, Irie T, et al. Importance of lymph node immune responses in MSI-H/dMMR colorectal cancer. JCI Insight. 2021;6:e137365. https://doi.org/10.1172/jci.insight.137365.
44. Ong ML, Schofield JB. Assessment of lymph node involvement in colorectal cancer. World J Gastrointest Surg. 2016;8:179–92. https://doi.org/10.4240/wjgs.v8.i3.179.

45. van de Laar BCT, Sikkenk DJ, Kats-Ugurlu G, de Groot DJA, Nagengast WB, Consten ECJ. Histopathological ultrastaging of mesocolic lymph nodes after colon cancer resection: a systematic review and meta-analysis. Crit Rev Oncol Hematol. 2026;218:105089. https://doi.org/10.1016/j.critrevonc.2025.105089.
46. Hirche C, Mohr Z, Kneif S, Doniga S, Murawa D, Strik M, et al. Ultrastaging of colon cancer by sentinel node biopsy using fluorescence navigation with indocyanine green. Int J Colorectal Dis. 2012;27:319–24. https://doi.org/10.1007/s00384-011-1306-5.
47. Johannesen KMB, Fiehn A-MK, Eiholm S. The topographical distribution of lymph node metastases in colon cancer resections. Ann Diagn Pathol. 2023;67:152205. https://doi.org/10.1016/j.anndiagpath.2023.152205.
48. Banipal GS, Stimec BV, Andersen SN, Edwin B, Nesgaard JM, Šaltytė Benth J, et al. Are metastatic central lymph nodes (D3 volume) in right-sided colon cancer a sign of systemic disease? A sub-group analysis of an ongoing multicenter trial. Ann Surg. 2024;279:648–56. https://doi.org/10.1097/SLA.0000000000006099.
49. Panaiotti L, Karachun A, Muravtseva A, Golovanova T, Khaetskaya M, Shkatov M, et al. Indocyanine green (ICG) fluorescence guided lymph node mapping for determination of resection margins in colon cancer: ISCAPE trial. Tech Coloproctol. 2025;29:179. https://doi.org/10.1007/s10151-025-03222-3.
50. Watanabe J, Ota M, Suwa Y, Ishibe A, Masui H, Nagahori K. Real-time indocyanine green fluorescence imaging-guided complete mesocolic excision in laparoscopic flexural colon cancer surgery. Dis Colon Rectum. 2016;59:701–5. https://doi.org/10.1097/DCR.0000000000000608.
51. Ueno H, Kim NK, Kim JC, Tsarkov P, Hohenberger W, Grützmann R, et al. Lymph node mapping-based optimal bowel-resection margin and central radicality in colon cancer surgery: an international, prospective, observational cohort study. ESMO Gastrointest Oncol. 2025;9:100231. https://doi.org/10.1016/j.esmogo.2025.100231.

Figures

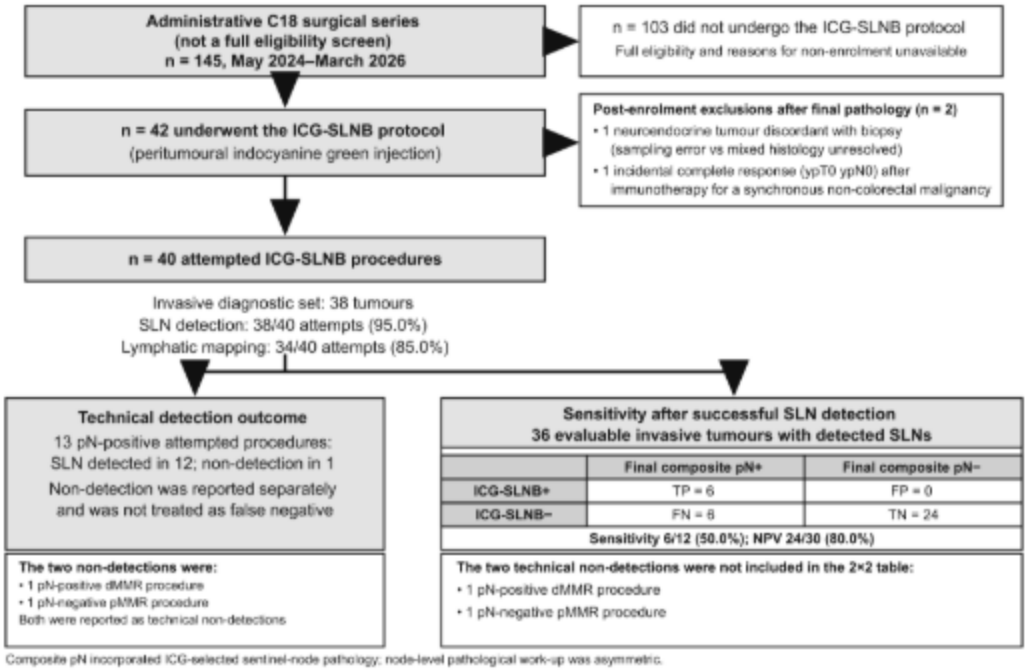


Figure 1

Combined STROBE cohort and STARD participant flow.

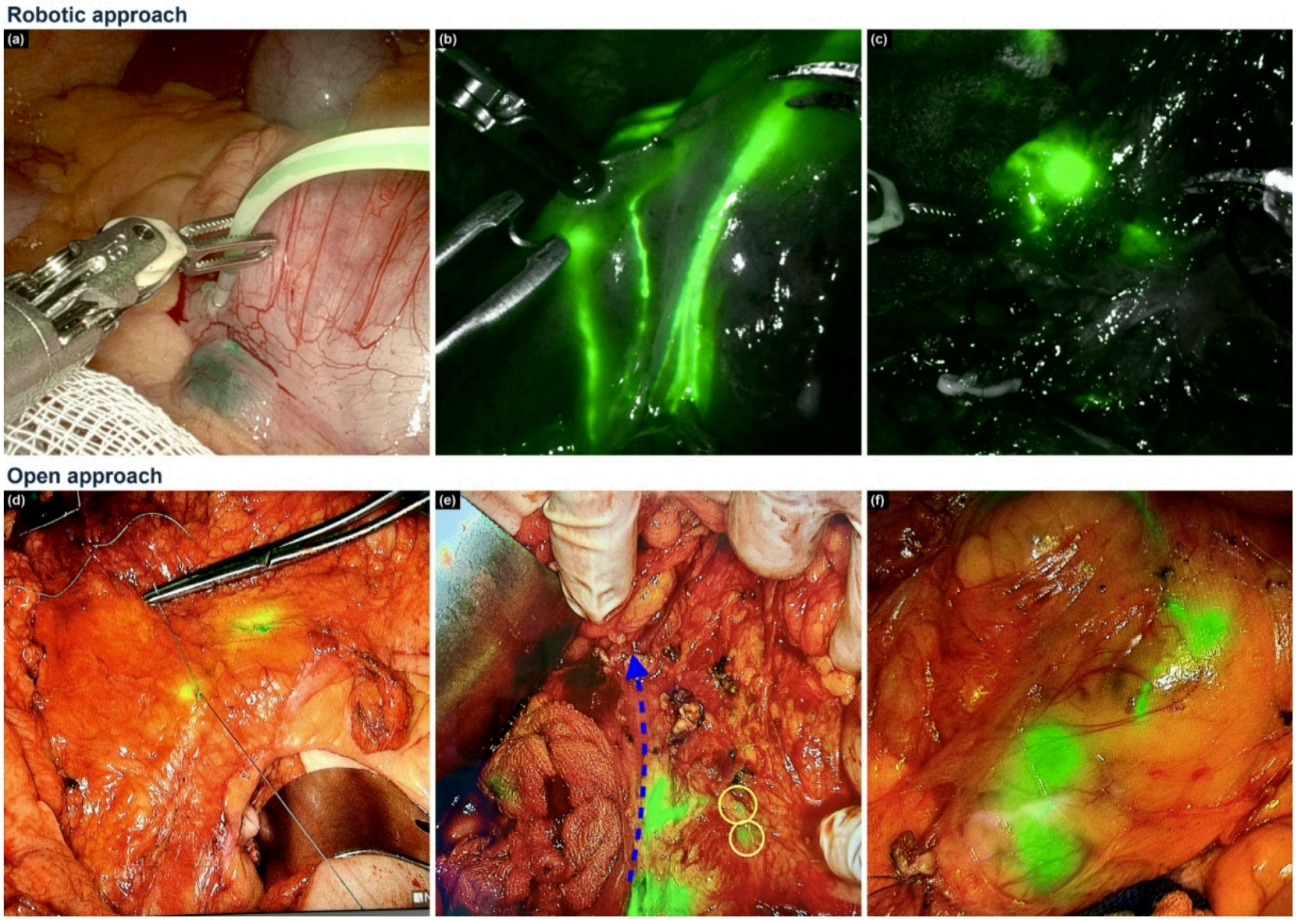


Figure 2

Intraoperative indocyanine green fluorescence-guided sentinel lymph node mapping in robotic and open colectomy.

(a–c) Robotic approach. (a) Subserosal peritumoural ICG injection. (b) Fluorescence-guided identification and clip marking of a sentinel lymph node (SLN). (c) Fluorescent SLN within the mesocolon.

(d–f) Open approach. (d) Suture marking of fluorescent SLNs. (e) Centrally located SLNs (yellow rings mark the fluorescent sentinel nodes). The blue arrow indicates the course of the superior mesenteric vein. (f) Fluorescent SLNs and lymphatic channels in a mesocolic location. ICG, indocyanine green; SLN, sentinel lymph node.

Supplementary Files

This is a list of supplementary files associated with this preprint. Click to download.

- Add3STARDchecklist.docx
- Add2STROBEchecklist.docx
- Add1.docx